Cell Host & Microbe
Article

The Double-Stranded RNA-Binding Protein PACT Functions as a Cellular Activator of RIG-I to Facilitate Innate Antiviral Response

Kin-Hang Kok,[1] Pak-Yin Lui,[1] Ming-Him James Ng,[1] Kam-Leung Siu,[1] Shannon Wing Ngor Au,[2] and Dong-Yan Jin[1,*]
[1]Department of Biochemistry and State Key Laboratory for Liver Research, Li Ka Shing Faculty of Medicine, The University of Hong Kong, Pokfulam, Hong Kong
[2]Department of Biochemistry, Faculty of Science, Chinese University of Hong Kong, Shatin, New Territories, Hong Kong
*Correspondence: dyjin@hku.hk
DOI 10.1016/j.chom.2011.03.007

SUMMARY

RIG-I, a virus sensor that triggers innate antiviral response, is a DExD/H box RNA helicase bearing structural similarity with Dicer, an RNase III-type nuclease that mediates RNA interference. Dicer requires double-stranded RNA-binding protein partners, such as PACT, for optimal activity. Here we show that PACT physically binds to the C-terminal repression domain of RIG-I and potently stimulates RIG-I-induced type I interferon production. PACT potentiates the activation of RIG-I by poly(I:C) of intermediate length. PACT also cooperates with RIG-I to sustain the activation of antiviral defense. Depletion of PACT substantially attenuates viral induction of interferons. The activation of RIG-I by PACT does not require double-stranded RNA-dependent protein kinase or Dicer, but is mediated by a direct interaction that leads to stimulation of its ATPase activity. Our findings reveal PACT as an important component in initiating and sustaining the RIG-I-dependent antiviral response.

INTRODUCTION

Host cells sense invading viruses and mobilize innate immune response to counteract their infection. Detection of viral nucleic acids by the cytoplasmic sensor RIG-I generates an activation signal which leads ultimately to the production of type I interferons (IFNs) that are important effectors in innate immunity (Yoneyama et al., 2004). RIG-I discriminates between viral and cellular RNAs by recognizing 5′-triphosphates and base-paired structures (Hornung et al., 2006; Pichlmair et al., 2006; Schlee et al., 2009b; Schmidt et al., 2009). On the other hand, RIG-I senses viral DNA in the cytosol (Choi et al., 2009) through multiple mechanisms, including the recognition of 5′-triphosphate RNA generated from DNA template by RNA polymerase III (Chiu et al., 2009). However, some double-stranded RNAs without 5′-triphosphates can also activate RIG-I (Hausmann et al., 2008; Schlee et al., 2009a). RIG-I is most efficiently activated by viruses, but the nature of viral RNA agonists bound to endogenous RIG-I during the course of infection has not been unequivocally determined (Baum et al., 2010; Rehwinkel et al., 2010). RIG-I is activated potently by unattached polyubiquitin chains (Zeng et al., 2010), but the physiological inducers of this activation are not understood. It also remains to be seen whether the action of RIG-I might require additional cellular partners and modifiers.

RIG-I is a DExD/H box RNA helicase bearing significant structural similarity with Dicer, an RNase III-type nuclease required for RNA interference (RNAi). Human Dicer requires dsRNA-binding protein partners TRBP and PACT for optimal activity in RNAi (Chendrimada et al., 2005; Haase et al., 2005; Lee et al., 2006; Kok et al., 2007). Surprisingly, a *C. elegans* protein named p110, which is an unrecognized homolog of RIG-I, was found to interact physically with PACT homolog RDE4 in an early study (Tabara et al., 2002). In addition, before the identification of RIG-I, PACT was also known to be capable of stimulating viral induction of type I IFNs (Iwamura et al., 2001). These findings prompted us to examine the interaction between human RIG-I and PACT as well as the implications in innate antiviral response.

RESULTS

PACT Interacts with RIG-I

We employed two different approaches to investigate the interaction of PACT and RIG-I. First, we performed coimmunoprecipitation experiments with lysates of transfected and untransfected HEK293 cells. For transfected cells expressing Myc-PACT and Flag-RIG-I, both proteins were found in the precipitates prepared separately with anti-Myc and anti-Flag (Figure 1A, lanes 2 and 3 compared to lane 1), and the formation of a RIG-I-PACT protein complex inside cells was confirmed. In contrast, Myc-PACT did not form a complex with Flag-TRAF3 (Figure 1A, lane 3), lending further support to the specificity of the interaction between PACT and RIG-I. Interestingly, only a fraction of RIG-I was seen to be associated with PACT. Likewise, only a subset of PACT bound to RIG-I. These results were compatible with the notion that the two multifunctional proteins might form functional complexes with other partners (Yoneyama et al., 2004; Kok et al., 2007).

When we repeated the coimmunoprecipitation experiment using mock-transfected and mock-infected A549 cells, RIG-I was not detected in either anti-PACT or anti-RIG-I precipitate (Figure 1B, lanes 2 and 3), indicating that the amount of RIG-I was too low in these cells. After induction of RIG-I expression

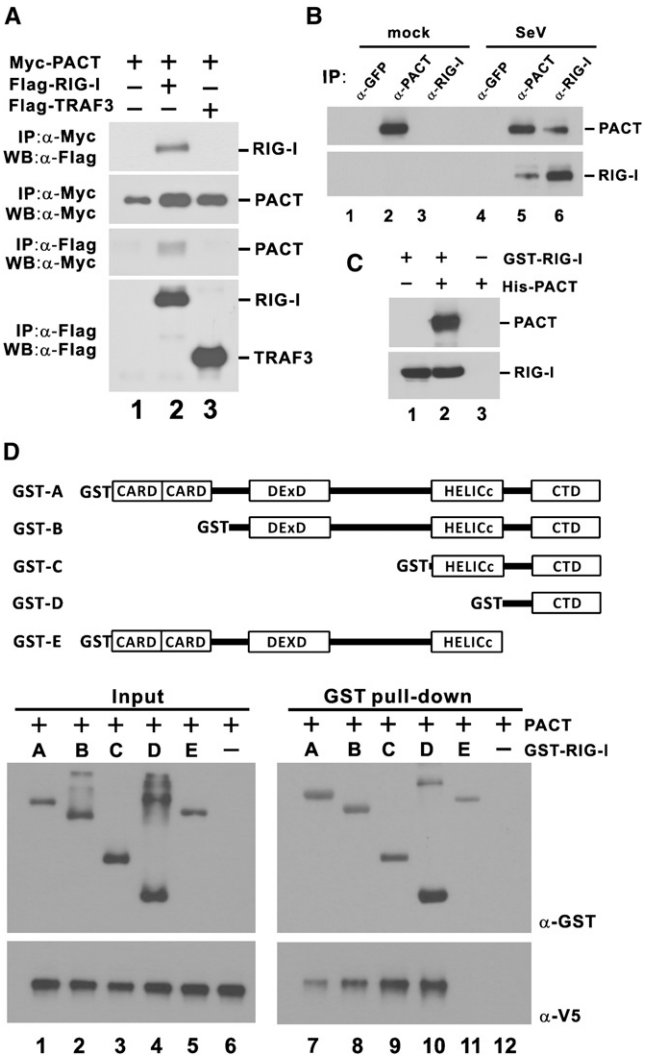

Figure 1. PACT Directly Interacts with RIG-I

(A) RIG-I and PACT were coimmunoprecipitated from lysates of transfected HEK293T cells. Cells were transfected with the indicated combinations of Myc-PACT, Flag-RIG-I, and Flag-TRAF3 expression plasmids. Reciprocal immunoprecipitation (IP) and western blotting (WB) were performed with the indicated antibodies.

(B) RIG-I and PACT were coimmunoprecipitated from lysates of untransfected A459 cells. Cells were mock infected or infected with 80 HA units of SeV for 24 hr. Immunoprecipitation was performed with the indicated antibodies. Endogenous PACT and RIG-I in the precipitates were probed with anti-PACT and anti-RIG-I.

(C) GST pull-down assay. GST-RIG-I and V5/His-PACT proteins purified to homogeneity were incubated for 1 hr and bound to glutathione beads. Bound proteins were analyzed with anti-His (upper panel) and anti-GST (lower panel).

(D) PACT binds to CTD of RIG-I. GST pull-down assay was performed with PACT and truncated mutants of RIG-I. The upper diagram depicts the domain organization of truncated mutants. Results are representative of three independent experiments.

by Sendai virus (SeV), RIG-I was found in the anti-PACT precipitate (Figure 1B, lane 5), and reciprocally, PACT was detected in the anti-RIG-I precipitate (Figure 1B, lane 6). Thus, endogenous PACT forms a complex with endogenous RIG-I in virus-infected cells.

Next, to rule out the possibility that the interaction between RIG-I and PACT is adapted through another protein, we carried out GST pull-down assay in vitro with purified recombinant proteins. His-PACT and GST-RIG-I proteins were expressed in the baculovirus-insect cell system and purified to homogeneity (see Figure S1 available online). Retention of purified His-PACT in the glutathione beads bound to purified GST-RIG-I (Figure 1C, lane 2) indicated a direct interaction between the two entities. Further analysis with truncated GST-RIG-I mutants revealed that the C-terminal repression domain (CTD) of RIG-I was sufficient for binding with PACT (Figure 1D, lane 10 compared to lanes 7–9 and 11), whereas the CARD and helicase domains were dispensable for this interaction. Nonspecific binding of GST to PACT was also excluded in light of the inability of GST-E to interact with PACT (Figure 1D, lanes 5 and 11). Together, our results confirmed the interaction between RIG-I and PACT both in cultured cells and in vitro.

PACT Is a Potent Activator of RIG-I

The interaction of PACT with the CTD of RIG-I might plausibly affect the activation of RIG-I. With this in mind, we went on to characterize the influence of PACT on RIG-I-induced activation of IFN-β production in HEK293 cells in which the expression of endogenous RIG-I was undetectable. We noted that enforced expression of PACT alone had no influence on the activity of IFN-β promoter (Figure 2A, bars 2–4). In contrast, coexpression of RIG-I and PACT resulted in substantial enhancement of RIG-I-induced activation of IFN-β promoter (Figure 2A, bars 6–8). The helicase activity of RIG-I was seemingly required for the activation of RIG-I by PACT, since the helicase-dead K270A mutant of RIG-I (Yoneyama et al., 2004) was not activated by PACT (Figure 2A, bars 10–12). Similar results were also obtained when another reporter driven by the IRF3-binding enhancer elements alone was used (Figure 2B), suggesting that the stimulatory effect was mediated through activation of IRF3. In further support of this, the formation of IRF3 dimer, which is the active form of IRF3, was observed in HEK293 cells expressing both RIG-I and PACT (Figure 2C, lanes 2 and 3 compared to lanes 1, 4, 5, and 8). Interestingly, IRF3 dimer was also detected when RIG-I was induced by IFN-β in PACT-expressing HEK293 cells (Figure 2C, lane 7 compared to lane 6). The stimulation of RIG-I-dependent activation of IRF3 by PACT was highly specific, since PACT did not potentiate RIG-I-induced activation of NF-κB (Figure S2A, bars 9–12 compared to bars 1–4 and 5–8). Notably, we also observed a similar stimulatory effect of PACT on MDA5- mediated activation of IFN-β promoter and IRF3 (Figure S2B, bars 1–4 and 5–8), but not on MDA5-inudced activation of NF-κB (bars 9–12). Although further experiments are required to fully characterize the impact of PACT on MDA5, our results did suggest that PACT might target the conserved CTD in RIG-I and MDA5. Consistent with the binding of PACT to the CTD of RIG-I (Figure 1C), PACT had no effect on RIG-IN containing the N-terminal CARD domain alone (Figure S2C, bars 5–8 compared to bars 9–12). Finally, facilitation of RIG-I-activated IFN production by PACT was also shown by direct measurement of the antiviral activity of IFNs. Only in HEK293 cells expressing both RIG-I and PACT, a large amount of IFN was produced leading to significant inhibition ($\sim 10^4$-fold less virus) of subsequent infection by a green fluorescent protein (GFP)-expressing vesicular stomatitis

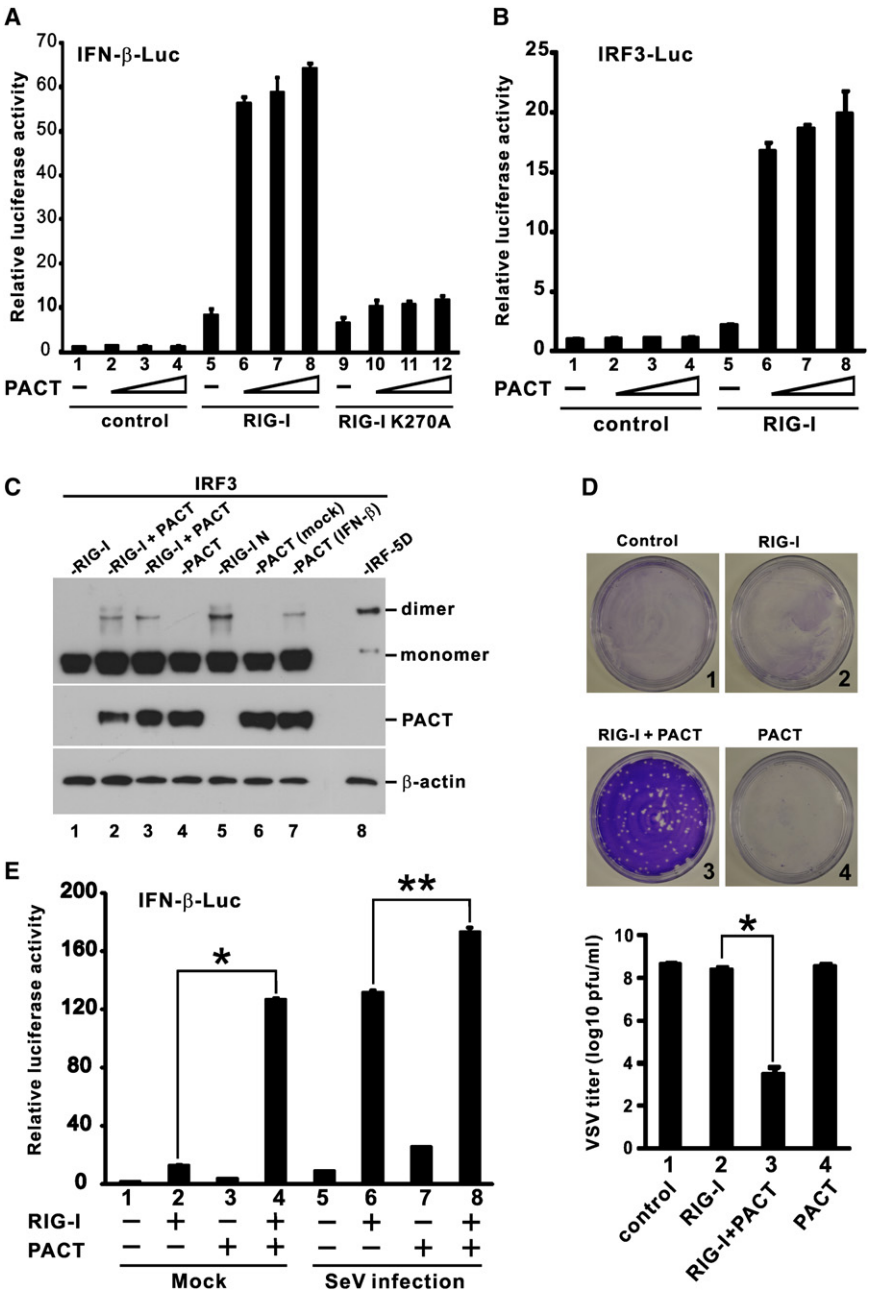

Figure 2. PACT Augments RIG-I-Induced Activation of IFN Production

(A and B) PACT enhances RIG-I-mediated activation of IFN-β promoter and IRF3. HEK293 cells were transfected with the indicated reporter and increasing amounts of PACT expression plasmid (50, 75, and 100 ng). Dual luciferase assay was carried out. Results represent three independent experiments, and error bars indicate SD.

(C) PACT stimulates RIG-I-induced dimerization of IRF3. HEK293 cells were transfected with expression plasmids for the indicated proteins. In lanes 2 and 3, two different doses of PACT were used. In lanes 5 and 8, constitutively active RIG-IN and IRF3-5D served as positive controls (Zhang et al., 2009). In lanes 6 and 7, transfected cells expressing PACT were either mock treated or treated with 1000 U/ml IFN-β. Cells were harvested at 28 hr posttransfection, and lysates were analyzed by native gel electrophoresis followed by western blotting with anti-Myc antibody. Dimeric and monomeric forms of IRF3 were indicated. The expression of PACT and β-actin was also verified. Similar results were also obtained from a duplicate experiment.

(D) PACT stimulates RIG-I-dependent induction of IFNs. HEK293 cells transfected with the indicated plasmids were infected at 28 hr posttransfection with VSV-GFP (moi = 1) for 1 hr. At 16 hr postinfection, viruses recovered from supernatants were quantitated by plaque formation assay in Vero cells. Data in the bar chart represent the mean ± SD of three independent experiments. *, the difference between the two groups is statistically very significant ($p = 0.0010$) by Student's t test.

(E) PACT facilitates viral activation of IFN-β promoter. At 28 hr posttransfection, HEK293 cells were infected with 80 HA units of SeV for 1 hr. Cells were harvested for dual luciferase assay at 10 hr postinfection. Data represent the mean ± SD of three independent experiments. * and **, the differences between the two groups are statistically significant ($p = 0.0016$ and $p = 0.011$, respectively) by Student's t test.

virus (VSV-GFP). VSV-GFP infection was essentially not affected in the other three groups because plenty of virus was recovered in the plaque formation assay (Figure 2D, panels/bars 1, 2, and 4 compared to panel/bar 3). Collectively, our data suggested that PACT exerts a stimulatory effect on the IFN-inducing activity of RIG-I through an interaction with the CTD.

We also assessed PACT-mediated potentiation of RIG-I activity in the context of viral infection. HEK293 cells transfected with different combinations of RIG-I and PACT plasmids were infected with SeV, and the IFN-β promoter activities were compared (Figure 2E). Overexpression of PACT alone stimulated viral induction of IFN-β production about 2-fold (Figure 2E, bar 7 compared to bar 5). This was probably due to PACT-mediated stimulation of RIG-I whose expression was induced during viral infection (Yoneyama et al., 2004). Overexpression of RIG-I alone potentiated viral activation of IFN-β promoter to a similar magnitude as in the presence of both PACT and RIG-I (Figure 2E, bar 6 compared to bar 4). PACT was also found to further augment RIG-I-induced activation of IFN-β promoter in virus-infected cells (Figure 2E, bar 8 compared to bar 6). These results demonstrated the cooperation between RIG-I and PACT in the activation of innate antiviral response in the context of SeV infection.

To shed light on the downstream effectors that transmit the activation signal triggered by PACT and RIG-I, we used a prevalidated siRNA to deplete the transcript of mitochondrial protein VISA, also known as MAVS or IPS1, which relays RIG-I signaling to IRF3 and NF-κB (Nakhaei et al., 2009). The effect of PACT and

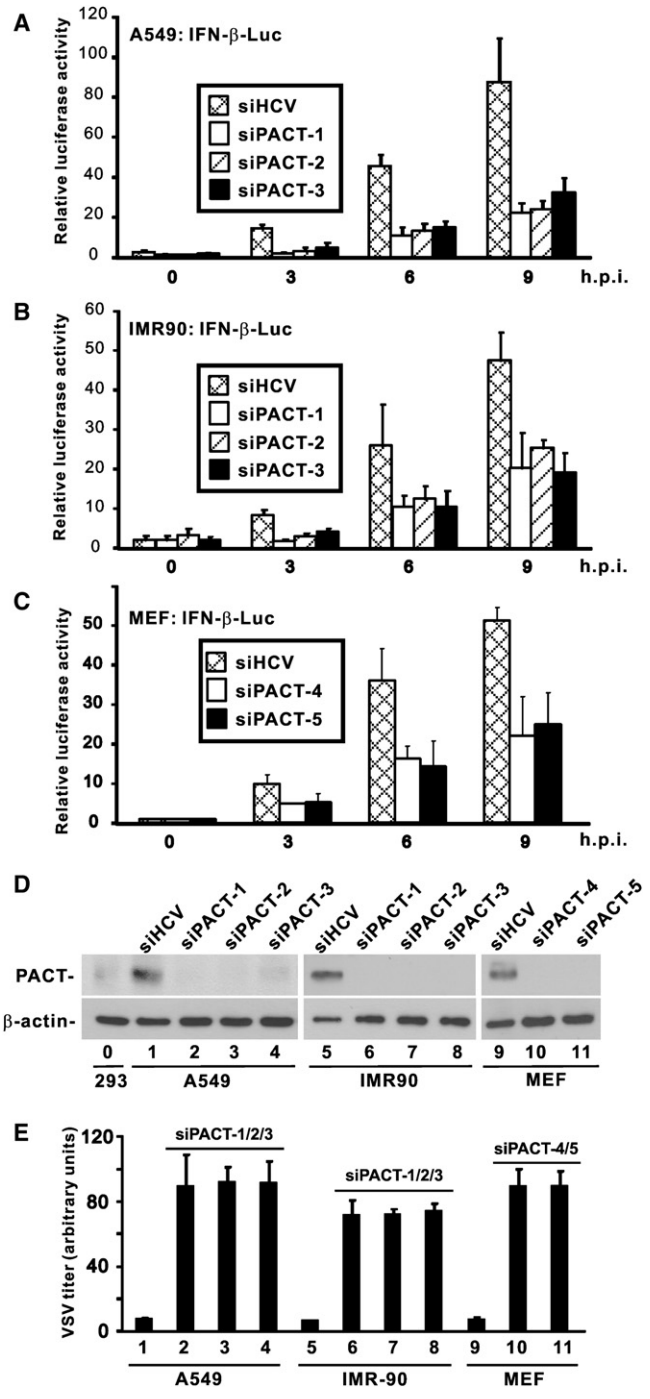

Figure 3. Silencing of PACT Inhibits Viral Induction of IFNs

(A–C) siRNA-transfected A549, IMR90, and MEF cells were infected with 80 HA units of SeV for 1 hr and harvested at different time points. siHCV is an irrelevant siRNA. Results are representative of three independent experiments, and error bars indicate SD; h.p.i., hours postinfection.

(D) Endogenous PACT protein in siRNA-transfected HEK293, A549, IMR90, and MEF cells was analyzed by western blotting at 72 hr posttransfection.

(E) siRNA-transfected A549, IMR90, and MEF cells were infected with 80 HA units of SeV at 72 hr posttransfection. At 1 hr postinfection, culture medium was transferred into untreated A549, IMR90, and MEF cells and incubated for another 1 hr. Cells were then infected with VSV-GFP (moi = 1) for 1 hr and analyzed by light and fluorescence microscopy at 12 hr after VSV-GFP infection (representative images are shown in Figure S3A). VSV titer was expressed as arbitrary units reflecting relative intensities of GFP fluorescence. Data presented represent the mean ± SD of three independent experiments.

RIG-I on IFN production, as indicated by reporter expression driven by IFN-β promoter or IRF3-binding enhancer elements, was substantially attenuated in VISA-depleted cells (Figure S2D, bars 3–4 compared to bars 1–2, and bars 7–8 compared to bars 5–6). This suggested the requirement of VISA for the activation of IFN-β production by PACT and RIG-I. Because different VISA-containing complexes might be used to activate IRF3 and NF-κB (Poeck et al., 2010), we checked for the recruitment of downstream effectors using coimmunoprecipitation. We found that a significant amount of endogenous TBK1 was recruited to the VISA complex in cells expressing PACT and RIG-I, whereas VISA-associated CARD9 was barely detectable in the same cells (Figure S2E, lane 2 compared to lane 1). In contrast, infection with SeV caused the recruitment of both TBK1 and CARD9 to the VISA complex (Figure S2E, lane 3) as expected. This indicated that TBK1 and CARD9 were differentially recruited to the VISA complex in cells expressing PACT and RIG-I. Because these two proteins are, respectively, required for IRF3 and NF-κB activation (Poeck et al., 2010), this might explain the specific effect of PACT on IRF3, but not NF-KB (Figure S2A).

We next investigated the role of PACT in viral induction of IFN-β using RNAi technology. Five siRNAs targeting human or mouse PACT transcript (siPACTs) were synthesized and introduced into two different cell lines, A549 and IMR90, as well as primary mouse embryonic fibroblasts (MEFs) (Figures 3A–3C). Compared to HEK293 cells, A549 cells abundantly expressed PACT protein (Figure 3D, lane 1 compared to lane 0). Whereas A549 is a lung adenocarcinoma epithelial cell line, IMR90 cells are normal diploid lung fibroblasts and MEF are primary cells derived from mouse embryo. The silencing effects of siPACTs in A549, IMR90, and MEF cells were verified by western blotting (Figure 3D). All five siPACTs were found to be highly effective and specific in counteracting PACT expression in human and mouse cells (Figure 3D, lanes 2–4, 6–8, and 10–11 compared to lanes 1, 5, and 9, respectively). In line with this almost complete knockdown of PACT, the induction of IFN-β promoter by SeV was significantly reduced at all three time points in siPACT-transfected A549, IMR90, and MEF cells (Figures 3A–3C). Consistent with this, transfer of culture medium from SeV-infected A549, IMR90, and MEF cells harboring siPACT into fresh untreated A549, IMR90, and MEF cells resulted in increased infectibility by VSV-GFP (Figure 3E, bars 2–4, 6–8, and 10–11 compared to bars 1, 5, and 9, respectively; also see Figure S3A for representative images, panels 6, 10, and 14 compared to panel 2, and panels 8, 12, and 16 compared to panel 4), indicative of an inhibition in IFN production. Consistently, when PACT was compromised, the ISRE-dependent transcriptional activity driving the expression of IFN-stimulated genes was also dampened, but in a delayed pattern (Figure S3B). In contrast, silencing of PACT had no influence on viral activation of NF-κB (Figure S3C). Direct measurement of the steady-state amounts of IFN-β and ISG15 transcripts in PACT-comprised A549 and MEF cells by quantitative RT-PCR confirmed an inhibition of viral activation of IFN-β and ISG15 (Figures S3D–S3G). These results consistently

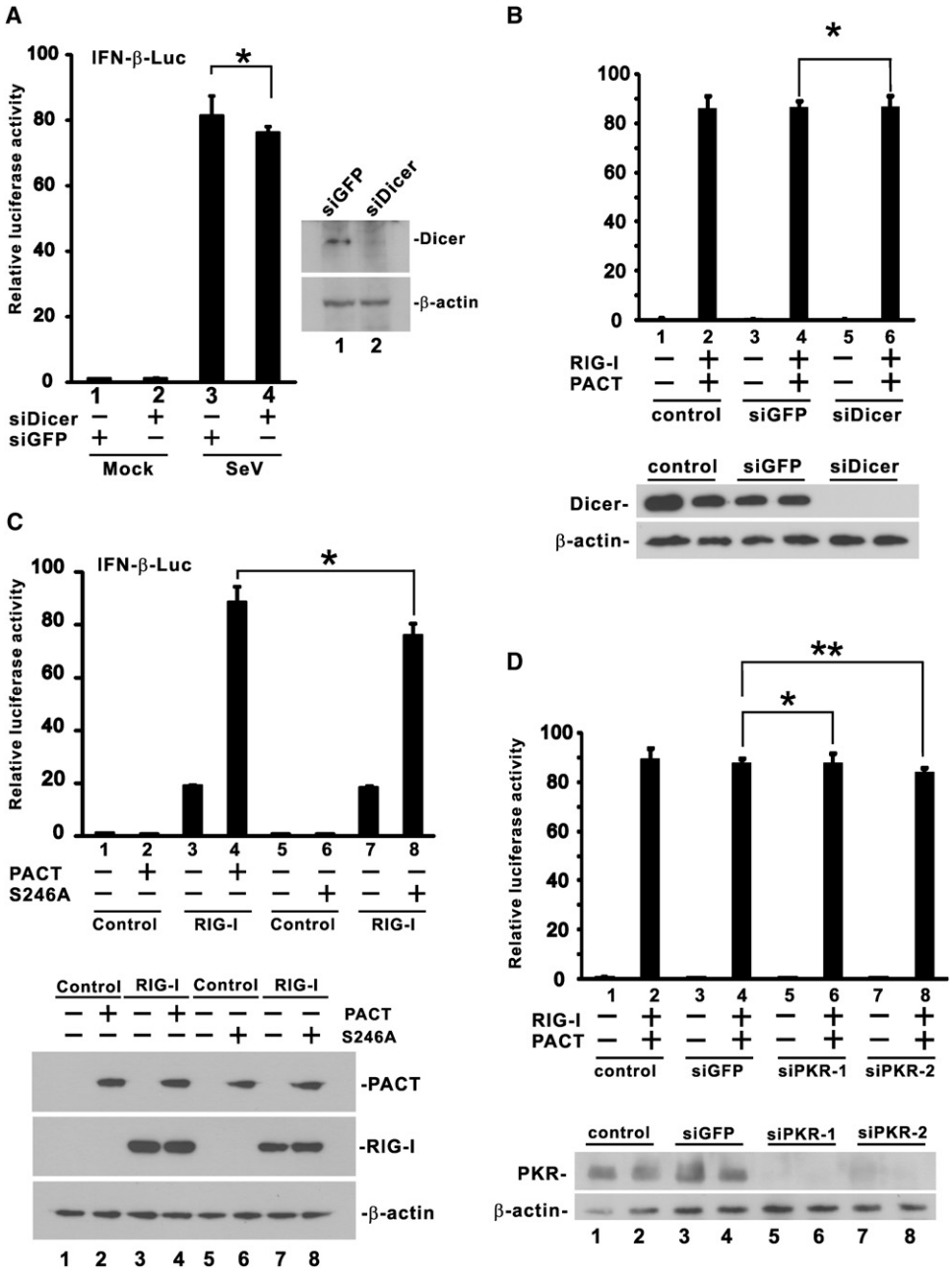

Figure 4. PACT-Mediated Activation of RIG-I Requires neither Dicer nor PKR

(A) A549 cells were transfected with siGFP or siDicer (Kok et al., 2007). Cells were infected with SeV (80 HA unit) for 1 hr. Dual luciferase assay was performed as in Figure 2. Dicer knockdown was verified by western blotting. *, the difference between the two groups is statistically insignificant (p = 0.42) by Student's t test.

(B) HEK293 cells were transfected with the indicated expression plasmids and siRNAs. Dual luciferase assay was carried out as in Figure 2. Dicer protein expression was verified by western blotting. Results are representative of three independent experiments and error bars indicate SD; *, the differences between the two groups are statistically insignificant (p = 0.64) by Student's t test.

(C) HEK293 cells were transfected with expression plasmid for PACT or its S246A mutant incapable of activating PKR (Peters et al., 2009a). Dual luciferase assay was carried out as in Figure 2. Protein expression was verified by western blotting. Results are representative of three independent experiments. *, the difference between the two groups is statistically insignificant (p = 0.085) by Student's t test.

(D) HEK293 cells were transfected with the indicated expression plasmids and siRNAs. Dual luciferase assay was carried out as in Figure 2. PKR protein expression was verified by western blotting. Results are representative of three independent experiments, and error bars indicate SD; * and **, the differences between the two groups are statistically insignificant (p = 0.69 and p = 0.62, respectively) by Student's t test.

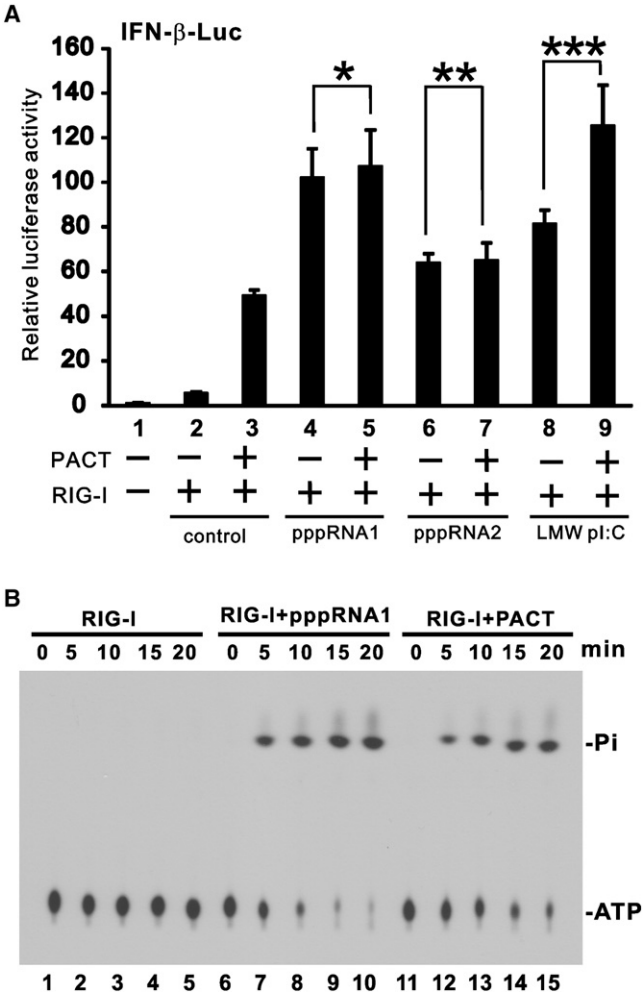

Figure 5. PACT Activates RIG-I Independently of 5′-Triphosphate RNA

(A) PACT does not potentiate 5′-triphosphate RNA-induced activation of RIG-I. HEK293 cells were transfected with the indicated expression plasmids and 5′-triphosphate RNA. Dual luciferase assay was performed as in Figure 2. Results represent the mean ± SD of three independent experiments. LMW pI:C, low-molecular-weight poly(I:C) of 0.2–1 kb in length. * and **, the differences between the two groups are statistically insignificant ($p = 0.70$ and $p = 0.84$, respectively) by Student's t test. ***, the difference between the two groups is statistically significant ($p = 0.04$) by Student's t test.

(B) PACT stimulates ATPase activity of RIG-I. Purified recombinant RIG-I protein (100 ng) was incubated with in vitro-transcribed pppRNA1 (100 ng) or purified recombinant PACT protein (100 ng) for 25 min at 37°C. The mixtures were further incubated with a reaction buffer containing 500 μM of [γ-^{32}P]-ATP. Reaction mixtures were quenched by adding formic acid at the indicated time points. Samples were resolved by thin-layer chromatography. Experiments were repeated for three times with similar results.

supported the requirement of PACT for full activation of innate antiviral response during viral infection.

PACT-Mediated Activation of RIG-I Does Not Require PKR or Dicer

PACT was initially cloned as a cellular binding partner and protein activator of dsRNA-dependent kinase PKR (Patel and Sen, 1998). On the other hand, PACT also interacted with and stimulated Dicer (Lee et al., 2006; Kok et al., 2007). While PKR was recently shown to enhance RIG-I-dependent activation of IFN production (McAllister and Samuel, 2009) and to modulate IFN mRNA stability in response to some viruses (Schulz et al., 2010), *Drosophila* Dicer-2 was also required for antiviral response (Deddouche et al., 2008). Thus, it would be of interest to investigate whether PACT-induced activation of RIG-I is mediated through PKR and Dicer. To determine the requirement for Dicer, we used siDicer to knockdown Dicer expression in SeV-infected cells. The specificity and effectiveness of this siDicer have been validated previously (Hutvágner et al., 2001). Since depletion of Dicer did not have a significant impact on SeV-induced activation of IFN-β production (Figure 4A, bar 4 compared to bar 3), which is dependent on RIG-I and PACT, Dicer unlikely played an important role in PACT-mediated regulation of antiviral response. Direct analysis of PACT-dependent activation of RIG-I in Dicer-depleted cells confirmed that Dicer is dispensable for the ability of PACT to stimulate RIG-I activity (Figure 4B, bar 6 compared to bars 2 and 4).

On the other hand, we made use of PACT mutant S246A defective for PKR activation (Peters et al., 2009a) to investigate the essentiality of PKR in PACT-induced activation of RIG-I. We noted that the S246A mutant exhibited RIG-I-activating activity comparable to wild-type PACT (Figure 4C, bar 8 compared to bar 4). In addition, when we used siPKR to knock down PKR expression (Figure 4D, lanes 5–8 compared to lanes 1–4), PACT-mediated activation of RIG-I was not affected (Figure 4D, bars 6 and 8 compared to bar 4). Hence, PKR was unlikely involved in the activation of RIG-I by PACT.

PACT Stimulates ATPase Activity of RIG-I

PACT binds directly to the CTD of RIG-I which is also activated upon binding with 5′-triphosphate dsRNA (Cui et al., 2008). Because PACT can bind to PKR and activate it in a dsRNA-independent fashion (Patel and Sen, 1998), we asked whether PACT might activate the activity of RIG-I in a similar manner. Indeed, when we introduced both PACT and 5′-triphosphate RNA agonist of RIG-I into HEK293 cells, an augmentation of IFN promoter activity was not observed (Figure 5A, bar 5 compared to bar 4, and bar 7 compared to bar 6). Interestingly, PACT was found to potentiate the activation of RIG-I by poly(I:C) of 0.2–1 kb in length (Figure 5A, bar 9 compared to bar 8). This intermediate-length poly(I:C) without 5′-triphosphate was previously known to be a potent activator of RIG-I (Schlee et al., 2009a), but the mechanism for its recognition by RIG-I remains elusive. The enhancement of its activation of RIG-I by PACT suggested that PACT might augment RNA activation of RIG-I in a 5′-triphosphate-independent manner. Consistent with the results of luciferase assay, incubation of purified recombinant proteins RIG-I and PACT in vitro led directly to activation of the intrinsic ATPase activity of RIG-I in the absence of 5′-triphosphate RNA (Figure 5B, lanes 11–15). In the same assay, 5′-triphosphate dsRNA was also capable of stimulating RIG-I ATPase (Figure 5B, lanes 6–10). We were not able to observe any synergistic RIG-I-stimulating effect between 5′-triphosphate RNA and PACT in our experimental setting (data not shown). Our results indicated that direct binding of PACT to the CTD of RIG-I sufficiently activated the virus sensor.

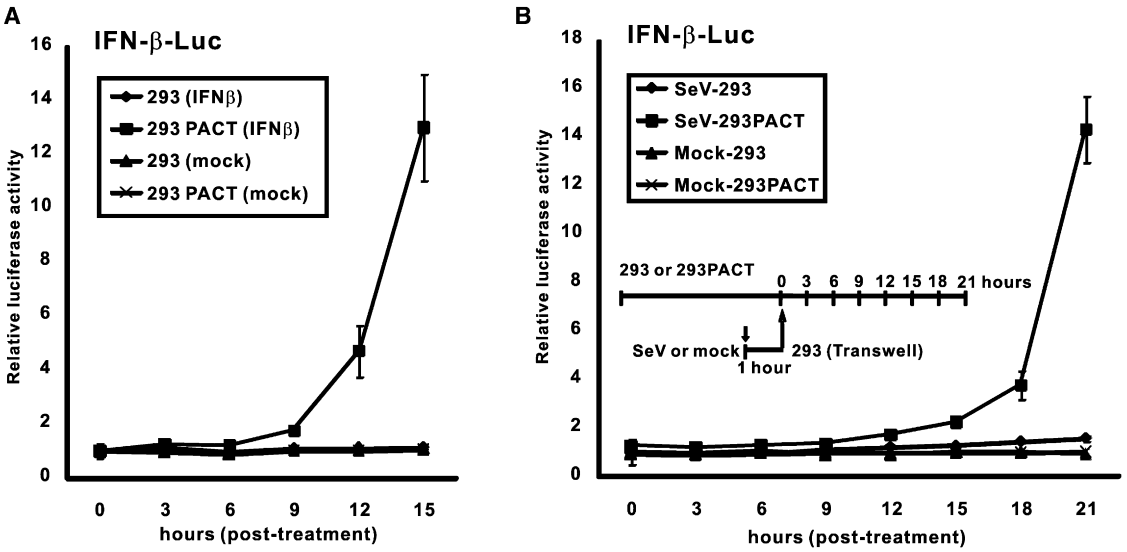

Figure 6. PACT Is Required for Signal Amplification in Antiviral Response

(A) HEK293 cell stably expressing PACT (293PACT) or not (293) were treated with IFN-β (1000 U/ml), harvested, and analyzed by dual luciferase assay.

(B) HEK293 cells were grown on transwells and then infected with SeV for 1 hr. After three washes, transwells were placed into the reporter-transfected 293 and 293PACT cells. Cells were incubated for the indicated duration, harvested, and analyzed by dual luciferase assay. Results are representative of three independent experiments, and error bars indicate SD.

PACT Cooperates with RIG-I to Sustain Antiviral Response

The activation of RIG-I by PACT in the absence of dsRNA prompted us to investigate whether PACT might play a role in amplifying the activation signal in innate antiviral response in uninfected cells adjacent to virus-infected cells. To this end, we treated HEK293 cells stably overexpressing PACT (293PACT) with IFN-β and followed the activation of IFN-β promoter in these cells. IFN-β is known to induce various IFN-stimulated genes including RIG-I (Yoneyama et al., 2004), which constitutes a positive feedback loop in the activation of IFN production. We found that IFN-β production was significantly activated only in IFN-β-treated 293PACT cells, but not in IFN-β-treated HEK293 cells (Figure 6A). Accordingly, we noted that the active IRF3 dimer was detected only in IFN-β-treated 293PACT cells, but not in IFN-β-treated HEK293 cells (Figure 2C, lane 7 compared to lane 6). Generally consistent with previous findings (Marié et al., 1998; Honda et al., 2006), our results suggested that induction of RIG-I alone by IFN-β was not sufficient for full activation of IFN production. Similar observations were also made if we grew SeV-infected HEK293 cells on transwells, which are transferable tissue culture inserts, and then placed them into uninfected PACT-expressing reporter cells (Figure 6B). Together, our data supported the notion that PACT is required for IFN-induced activation of IFN production in neighboring uninfected cells. In other words, PACT is an essential component in a positive feedback loop, and it cooperates with RIG-I to sustain the innate antiviral response.

One related question concerns the activation of PACT expression, which might be important in antiviral response. Particularly, it is of interest to see whether the expression of PACT is transcriptionally induced by RIG-I, IFN-β, or viral infection. To address this issue, we cloned the PACT promoter and assessed its response to RIG-IN or IRF3 (Figure S4A). Whereas both RIG-IN and IRF3 potently activated IFN-β promoter, they had minimal effect on the promoter of PACT. Unlike RIG-I and ISG15, whose expression was significantly induced by IFN-β or SeV infection, the steady-state levels of PACT mRNA and protein remained unchanged in IFN-treated or SeV-infected cells (Figures S4B and S4C). Thus, PACT expression was not induced by IFNs or viral infection. Taken together, PACT plays a role in initiating and sustaining RIG-I-induced antiviral response in both infected and uninfected cells (Figure 7). Plausibly, PACT might be naturally activated in uninfected cells through an as-yet-unknown mechanism. This activation effect was mimicked by the overexpression of PACT in our experiments presented in Figure 6.

DISCUSSION

In this study, we characterized dsRNA-binding protein PACT to be a binding partner and potent activator of DExD/H box helicase RIG-I (Figures 1 and 2). RNAi depletion of PACT led to inhibition of virus-induced and RIG-I-dependent activation of IFN production (Figure 3). The stimulation of RIG-I by PACT did not require PKR or Dicer (Figure 4), but was mediated through a direct interaction with the CTD of RIG-I leading to activation of ATPase activity (Figure 5) and plausibly a conformational change associated with the recruitment of downstream effectors. PACT facilitated RNA activation of RIG-I in a 5′-triphosphate-independent manner (Figure 5). PACT activation of RIG-I is also required for amplification of activation signal in innate immunity (Figures 6 and 7).

Our work identified another component in innate antiviral response. This is consistent with the finding that PACT stimulated viral induction of IFN-β (Iwamura et al., 2001). In addition, previous RNAi knockdown experiments in mice also suggested

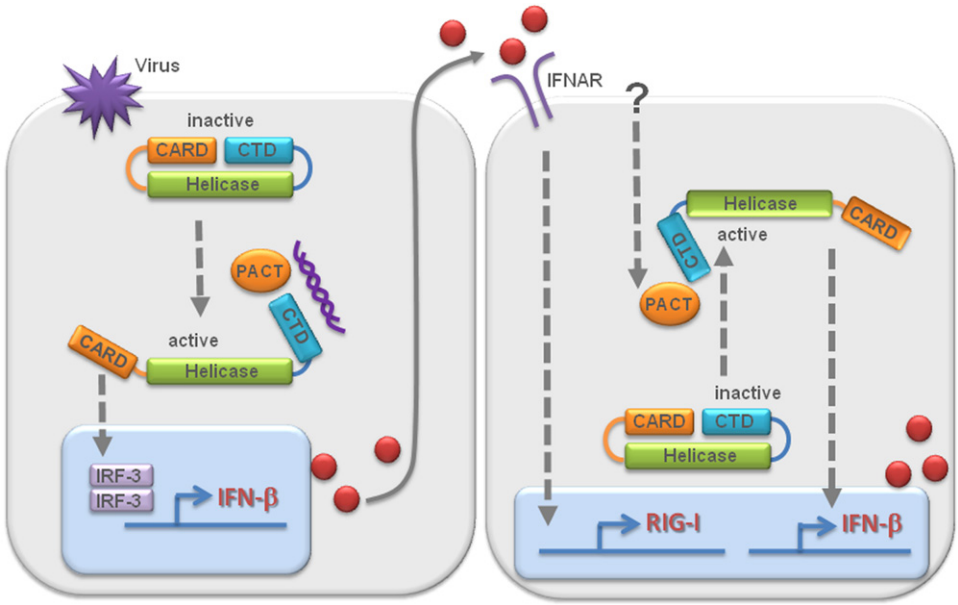

Figure 7. A Working Model for the Role of PACT in Initiating and Sustaining RIG-I-Induced Antiviral Response
IFNAR, IFN-α/β receptor. PACT might be activated through an as-yet-unknown mechanism in uninfected cells.

that compromising PACT sensitized cells to inflammatory cytokines and viral infection (Bennett et al., 2006). *Pact* knockout in mice created by one group through complete deletion of coding sequence turned out to be lethal (Bennett et al., 2008). In contrast, *Pact* null mice made by another group through removal of exon 8 coding for C-terminal of PACT showed developmental defects in hearing and pituitary function (Rowe et al., 2006; Peters et al., 2009b), but it remains to be clarified whether a truncated PACT protein that might be expressed in some tissues and cells of these mice could be functional, as in the case of *Drosophila* homolog of PACT named Loqs-PD (Hartig et al., 2009; Zhou et al., 2009). In this connection, further analyses are required to elucidate the physiological function of PACT in innate immunity and RNAi in animal model.

Although enzymatically inactive RIG-I was previously demonstrated to be able to activate IFN production (Bamming and Horvath, 2009), RIG-I is a ligand-dependent ATPase, and the ATPase activity was shown to be required for RNA-induced conformational change of RIG-I (Takahasi et al., 2008) and sensitization of RIG-I for further activation by unattached polyubiquitin chains (Zeng et al., 2010). Intriguingly, the unattached polyubiquitin chains can interact with and further activate RIG-IN lacking the CTD, but they were unable to activate an ATPase-dead mutant of RIG-I (Zeng et al., 2010). In line with some of these reports, our finding that PACT can sufficiently activate the ATPase activity of RIG-I supports the importance of ATPase activity in RIG-I activation. Further investigations are required to elucidate whether and how PACT interaction with RIG-I might affect the conformation of RIG-I or the interaction of the N-terminal domain of RIG-I with unattached polyubiquitin chains.

PACT can physically interact with viral antagonists of IFN such as influenza A virus NS1 (Li et al., 2006) and herpes simplex virus Us11 (Peters et al., 2002). The crucial role of PACT in facilitating RIG-I-dependent antiviral response suggested that PACT might serve as another regulatory point on which different viral proteins converge to circumvent host defense. Further investigations are underway in our laboratory to elucidate the mechanisms by which viral proteins inhibit the function of PACT and RIG-I.

A paralog of PACT termed TRBP was originally identified and characterized by its high affinity for TAR, a hairpin RNA encoded by human immunodeficiency virus type 1 (Gatignol et al., 1991). Although both PACT and TRBP bind to PKR and have three similar dsRNA-binding domains, TRBP exerts an inhibitory effect on PKR (Park et al., 1994). In sharp contrast, both TRBP and PACT interact simultaneously with Dicer and are required for Dicer function in RNAi (Kok et al., 2007). It will be of particularly great interest to elucidate whether TRBP also interacts with and modulates RIG-I activity. Our preliminary results suggested that TRBP neither stimulates RIG-I nor forms a triple complex with PACT and RIG-I (data not shown). Nevertheless, the interaction of PACT or TRBP with RIG-I and other RIG-I-like virus sensors, MDA5 and LGP2 (Satoh et al., 2010), merits further analysis. One emerging concept is that PACT might serve as a multiuse switch in several dsRNA-dependent signaling pathways by engaging different partners. Thus, it is of pivotal importance to shed light on how PACT interacts with its partners to coordinate its modulatory function on RIG-I, PKR, and Dicer.

Although PACT could activate RIG-I in vitro in the absence of RNA (Figure 5), PACT is a dsRNA-binding protein that can bind to RNA ligands of RIG-I. The RNA-binding properties of PACT, TRBP, and other related partners of Dicer are influential in Dicer function (Parker et al., 2008). In support of a role of PACT in ligand-induced activation of RIG-I, PACT was found to enhance the activation of RIG-I by intermediate-length poly(I:C) in a 5′-triphosphate-independent manner (Figure 5A). Because PACT can bind directly to poly(I:C) (Patel and Sen, 1998), it will be of interest to see whether and how PACT might select or concentrate

particular RNAs such as poly(I:C) and transfer them to RIG-I and MDA5. Compared to known RIG-I agonists including 5′-triphosphate RNA, viruses activate RIG-I much more potently and persistently (Nakhaei et al., 2009). It is therefore plausible that naturally occurring agonists of RIG-I generated during the course of viral infection might be more powerful. However, the identity of these natural agonists remains controversial (Baum et al., 2010; Rehwinkel et al., 2010). It is still an open question as to whether PACT might recognize any of these agonists other than 5′-triphosphate RNA and facilitate their activation of RIG-I. Our preliminary analysis of defective interfering RNAs generated during the course of SeV infection revealed that PACT could potentiate the activation of IFN production by some of these defective interfering RNAs (data not shown). Further characterization of the RIG-I ligands and their interaction with PACT in infected cells might shed light on the mechanism through which PACT stimulates viral induction of type I IFNs (Figure 2 and Iwamura et al., 2001).

We found that PACT and RIG-I preferentially activate IRF3, but not NF-κB (Figure S2A). We further correlated PACT-induced activation of RIG-I with strong recruitment of TBK1, but not CARD9, to the VISA-containing complex (Figure S2E). Our findings are consistent with the notion that RIG-I signaling might bifurcate or trifurcate at the level of VISA complex formation (Poeck et al., 2010). Although VISA is required for both IRF3 and NF-κB activation, it is not too surprising that upstream signals might selectively induce the formation of particular VISA-containing complex to impinge on IRF3 only. Some activators of RIG-I and VISA signaling, such as DDX3 and mitofusin 1, are actually not known to activate NF-κB (Schröder et al., 2008; Onoguchi et al., 2010). Exactly how PACT and other signals fine-tune the activity of RIG-I leading to differential activation of IRF3 and NF-κB remains to be elucidated.

EXPERIMENTAL PROCEDURES

Plasmids

Expression plasmid for Flag-RIG-I (pEF-flagRIG-I) and reporter construct pIFN-β-Luc were kindly provided by Takashi Fujita (Yoneyama et al., 2004). RIG-IN expression plasmid was constructed by PCR subcloning a DNA fragment encoding the N-terminal CARD region (1–284 amino acids) of RIG-I into pCMVtag2B vector (Stratagene). Myc-PACT expression plasmid has been described (Kok et al., 2007). pIRF3-Luc contains three tandem copies of the IRF3-binding site in IFN-β promoter. Baculoviral transfer vector pAcGHLT expressing full-length RIG-I was provided by Takashi Fujita (Cui et al., 2008). RIG-I-truncated mutants B-E comprise amino acids 258–926, 606–926, 742–926, and 1–741, respectively (Figure 1C). p3800-Luc reporter was constructed by inserting a PCR fragment containing the PACT promoter region (−3800 to +1) into pGL3.

Antibodies

Antibodies used in immunoprecipitation were mouse anti-Flag (M2; Sigma), mouse anti-Myc (9E10; Roche), and mouse anti-VISA (E3; Santa-Cruz). Antibodies for western blotting included mouse anti-Flag (M5; Sigma), rabbit anti-Myc (A-14; Santa Cruz), mouse anti-GST (B-14; Santa Cruz), mouse anti-V5 (Invitrogen), mouse anti-RIG-I (D14G6, Cell Signaling), mouse anti-TBK1 (108A429, Enzo), rabbit anti-Dicer (H-212; Santa Cruz), and rabbit anti-CARD9 (Enzo).

Protein and RNA Analysis

Western blotting, immunoprecipitation, GST pull-down assay, dual luciferase reporter assay, fluorescence microscopy, and RT-PCR were performed as described (Kok and Jin, 2006; Kok et al., 2007). Quantitative real-time PCR was carried out in StepOne Real-Time PCR System (Applied Biosystems). Quantitation of target mRNA expression was achieved with the comparative Ct method. Relative expression level of target mRNA was calculated from $2^{-\Delta Ct}$.

Viral Infection and Plaque Formation Assay

HEK293, A549, Vero, IMR90, and MEF cells were cultured as described (Kok et al., 2007; Siu et al., 2009). Primary MEF cells were generated from E13 embryos of wild-type mouse in C57BL/6J background. SeV (Cantell strain) was purchased from American Type Culture Collection. In all experiments, 80 HA units of SeV was added to each well in a 12-well plate. GFP version of vesicular stomatitis virus (VSV-GFP) was kindly provided by Jacques Perrault, Brian Lichty, and Dominique Garcin (Ostertag et al., 2007; Brown et al., 2009). For plaque formation assay, Vero cells were infected with serial 10-fold dilutions of the virus in culture medium. Infected Vero cells were then overlaid with 1:1 culture medium containing 1% agarose. At 16 hr postinfection, cells were fixed with 1:1 methanol-ethanol and stained with 0.05% crystal violet.

RNA Transfection

HEK293, A549, IMR90, and MEF cells were transfected with 50 nM RNA using Lipofectamine 2000 (Invitrogen). Target sequences of siPACT-1, siPACT-2, siPACT-3, siPACT-4, siPACT-5, siPKR-1, siPKR-2, siGFP, siDicer, siVISA, and siHCV were 5′-GAGAGAAUAUACUACAAUU-3′, 5′-GCAGAGGCUGCCAUAAACA-3′, 5′-GCCUCCUUAGUAUUCCAAA-3′, 5′-GAGGGAAUACACCACGAUC-3′, 5′-CACCGAUUCAGGUAUUGCA-3′, 5′-GACGGAAAGACUUACGUUA-3′, 5′-GGAACUUUGCGAUACAUGA-3′, 5′-GCAAGCUGACCCUGAAGUU-3′, 5′-UGCUUGAAGCAGCUCUGGA-3′, 5′-CAAGACCUAUAAGUAUAUC-3′, and 5′-CCUCGAGGUAGACGUCAGC-3′, respectively. pppRNA1 was a 5′-triphosphate dsRNA of 341 bp corresponding to the 5′ end of hepatitis C virus genome. It was prepared by in vitro transcription and annealing as described (Schlee et al., 2009b). pppRNA2, alternatively named as hp2.2 in a previous study (Schmidt et al., 2009), was an in vitro-transcribed RNA with 5′-triphosphate and base-paired structure. Low-molecular-weight poly(I:C) with an average size of 0.2–1 kb was purchased from InvivoGen.

Protein Purification

Preparation of baculoviruses and transduction of Sf9 insect cells were performed using the protocols provided by BD Biosciences. GST-RIG-I and V5/His-PACT were coexpressed in Sf9 cells. Recombinant baculoviruses were then amplified to obtain a high-titer stock solution, approximately 10^7 virus particles/ml as measured by plaque assay. For protein expression, Sf9 cells were infected with viruses (moi = 1), and the proteins expressed were harvested at 3 days postinfection and were purified using glutathione (Amersham) and nickel (QIAGEN) beads.

ATPase Assay

Recombinant RIG-I protein (100 ng) purified to homogeneity was incubated with in vitro-transcribed dsRNA (100 ng) prepared as previously described (Kok et al., 2007) or with purified recombinant PACT protein (100 ng) for 25 min at 37°C. The mixtures were further incubated in a reaction buffer containing 500 μM [γ-^{32}P]ATP, 50 mM Tris-acetate (pH 6.0), 5 mM dithiothreitol, and 1.5 mM $MgCl_2$. Reaction mixtures were quenched by adding formic acid to a final concentration of 1 M at different time points. Samples were resolved by thin-layer chromatography on polyethyleneimine cellulose F plates (Merck) in a buffer containing 1 M formic acid and 0.5 M LiCl.

SUPPLEMENTAL INFORMATION

Supplemental Information includes four figures and can be found with this article at doi:10.1016/j.chom.2011.03.007.

ACKNOWLEDGMENTS

This work was supported by Hong Kong Research Fund for the Control of Infectious Diseases (HSI/Lab-17 and 10091202) and Hong Kong Research Grants Council (HKU 7677/10M and HKU 7/CRF/09). We thank Takashi Fujita, Dominique Garcin, Greg Hannon, Brian Lichty, and Jacques Perrault for gifts of reagent; and Abel Chun, Kuan-Teh Jeang, Allan Lau, Ting Lei, Vincent Tang, and Chi-Ming Wong for critical reading of the manuscript. K.-H.K., S.W.N.A.,

and D.-Y.J. designed the study. K.-H.K., P.-Y.L., M.-H.J.N., and K.-L.S. performed experiments. K.-H.K., S.W.N.A., and D.-Y.J. analyzed the data. K.-H.K. and D.-Y.J. wrote the paper.

Received: October 5, 2010
Revised: December 14, 2010
Accepted: March 4, 2011
Published: April 20, 2011

REFERENCES

Bamming, D., and Horvath, C.M. (2009). Regulation of signal transduction by enzymatically inactive antiviral RNA helicase proteins MDA5, RIG-I, and LGP2. J. Biol. Chem. *284*, 9700–9712.

Baum, A., Sachidanandam, R., and García-Sastre, A. (2010). Preference of RIG-I for short viral RNA molecules in infected cells revealed by next generation sequencing. Proc. Natl. Acad. Sci. USA *107*, 16303–16308.

Bennett, R.L., Blalock, W.L., Abtahi, D.M., Pan, Y., Moyer, S.A., and May, W.S. (2006). RAX, the PKR activator, sensitizes cells to inflammatory cytokines, serum withdrawal, chemotherapy, and viral infection. Blood *108*, 821–829.

Bennett, R.L., Blalock, W.L., Choi, E.J., Lee, Y.J., Zhang, Y., Zhou, L., Oh, S.P., and May, W.S. (2008). RAX is required for fly neuronal development and mouse embryogenesis. Mech. Dev. *125*, 777–785.

Brown, C.W., Stephenson, K.B., Hanson, S., Kucharczyk, M., Duncan, R., Bell, J.C., and Lichty, B.D. (2009). The p14 FAST protein of reptilian reovirus increases vesicular stomatitis virus neuropathogenesis. J. Virol. *83*, 552–561.

Chendrimada, T.P., Gregory, R.I., Kumaraswamy, E., Norman, J., Cooch, N., Nishikura, K., and Shiekhattar, R. (2005). TRBP recruits the Dicer complex to Ago2 for microRNA processing and gene silencing. Nature *436*, 740–744.

Chiu, Y.H., Macmillan, J.B., and Chen, Z.J. (2009). RNA polymerase III detects cytosolic DNA and induces type I interferons through the RIG-I pathway. Cell *138*, 576–591.

Choi, M.K., Wang, Z., Ban, T., Yanai, H., Lu, Y., Koshiba, R., Nakaima, Y., Hangai, S., Savitsky, D., Nakasato, M., et al. (2009). A selective contribution of the RIG-I-like receptor pathway to type I interferon responses activated by cytosolic DNA. Proc. Natl. Acad. Sci. USA *106*, 17870–17875.

Cui, S., Eisenächer, K., Kirchhofer, A., Brzózka, K., Lammens, A., Lammens, K., Fujita, T., Conzelmann, K.-K., Krug, A., and Hopfner, K.-P. (2008). The C-terminal regulatory domain is the RNA 5′-triphosphate sensor of RIG-I. Mol. Cell *29*, 169–179.

Deddouche, S., Matt, N., Budd, A., Mueller, S., Kemp, C., Galiana-Arnoux, D., Dostert, C., Antoniewski, C., Hoffmann, J.A., and Imler, J.L. (2008). The DExD/H-box helicase Dicer-2 mediates the induction of antiviral activity in *Drosophila*. Nat. Immunol. *9*, 1425–1432.

Gatignol, A., Buckler-White, A., Berkhout, B., and Jeang, K.T. (1991). Characterization of human TAR RNA-binding protein that activates the HIV-1 LTR. Science *251*, 1597–1600.

Haase, A.D., Jaskiewicz, L., Zhang, H., Lainé, S., Sack, R., Gatignol, A., and Filipowicz, W. (2005). TRBP, a regulator of cellular PKR and HIV-1 virus expression, interacts with Dicer and functions in RNA silencing. EMBO Rep. *6*, 961–967.

Hartig, J.V., Esslinger, S., Böttcher, R., Saito, K., and Förstemann, K. (2009). Endo- siRNAs depend on a new isoform of loquacious and target artificially introduced, high-copy sequences. EMBO J. *28*, 2932–2944.

Hausmann, S., Marq, J.B., Tapparel, C., Kolakofsky, D., and Garcin, D. (2008). RIG-I and dsRNA-induced IFNβ activation. PLoS ONE *3*, e3965. 10.1371/journal.pone.0003965.

Honda, K., Takaoka, A., and Taniguchi, T. (2006). Type I interferon gene induction by the interferon regulatory factor family of transcription factors. Immunity *25*, 349–360.

Hornung, V., Ellegast, J., Kim, S., Brzózka, K., Jung, A., Kato, H., Poeck, H., Akira, S., Conzelmann, K.-K., Schlee, M., et al. (2006). 5′-Triphosphate RNA is the ligand for RIG-I. Science *314*, 994–997.

Hutvágner, G., McLachlan, J., Pasquinelli, A.E., Bálint, E., Tuschl, T., and Zamore, P.D. (2001). A cellular function for the RNA-interference enzyme Dicer in the maturation of the let-7 small temporal RNA. Science *293*, 834–838.

Iwamura, T., Yoneyama, M., Koizumi, N., Okabe, Y., Namiki, H., Samuel, C.E., and Fujita, T. (2001). PACT, a double-stranded RNA binding protein acts as a positive regulator for type I interferon gene induced by Newcastle disease virus. Biochem. Biophys. Res. Commun. *282*, 515–523.

Kok, K.H., and Jin, D.Y. (2006). Influenza A virus NS1 protein does not suppress RNA interference in mammalian cells. J. Gen. Virol. *87*, 2639–2644.

Kok, K.H., Ng, M.H.J., Ching, Y.P., and Jin, D.Y. (2007). Human TRBP and PACT interact with each other and associate with Dicer to facilitate the production of siRNA. J. Biol. Chem. *282*, 17649–17657.

Lee, Y., Hur, I., Park, S.-Y., Kim, Y.-K., Suh, M.R., and Kim, V.N. (2006). The role of PACT in the RNA silencing pathway. EMBO J. *25*, 522–532.

Li, S., Min, J.Y., Krug, R.M., and Sen, G.C. (2006). Binding of the influenza A virus NS1 protein to PKR mediates the inhibition of its activation by either PACT or double-stranded RNA. Virology *349*, 13–21.

Marié, I., Durbin, J.E., and Levy, D.E. (1998). Differential viral induction of distinct interferon-α genes by positive feedback through interferon regulatory factor-7. EMBO J. *17*, 6660–6669.

McAllister, C.S., and Samuel, C.E. (2009). The RNA-activated protein kinase enhances the induction of interferon-β and apoptosis mediated by cytoplasmic RNA sensors. J. Biol. Chem. *284*, 1644–1651.

Nakhaei, P., Genin, P., Civas, A., and Hiscott, J. (2009). RIG-I-like receptors: sensing and responding to RNA virus infection. Semin. Immunol. *21*, 215–222.

Onoguchi, K., Onomoto, K., Takamatsu, S., Jogi, M., Takemura, A., Morimoto, S., Julkunen, I., Namiki, H., Yoneyama, M., and Fujita, T. (2010). Virus-infection or 5′ppp-RNA activates antiviral signal through redistribution of IPS-1 mediated by MFN1. PLoS Pathog. *6*, e1001012. 10.1371/journal.ppat.1001012.

Ostertag, D., Hoblitzell-Ostertag, T.M., and Perrault, J. (2007). Overproduction of double-stranded RNA in vesicular stomatitis virus-infected cells activates a constitutive cell-type-specific antiviral response. J. Virol. *81*, 503–513.

Park, H., Davies, M.V., Langland, J.O., Chang, H.W., Nam, Y.S., Tartaglia, J., Paoletti, E., Jacobs, B.L., Kaufman, R.J., and Venkatesan, S. (1994). TAR RNA-binding protein is an inhibitor of the interferon-induced protein kinase PKR. Proc. Natl. Acad. Sci. USA *91*, 4713–4717.

Parker, G.S., Maity, T.S., and Bass, B.L. (2008). dsRNA binding properties of RDE-4 and TRBP reflect their distinct roles in RNAi. J. Mol. Biol. *384*, 967–979.

Patel, R.C., and Sen, G.C. (1998). PACT, a protein activator of the interferon-induced protein kinase, PKR. EMBO J. *17*, 4379–4390.

Peters, G.A., Khoo, D., Mohr, I., and Sen, G.C. (2002). Inhibition of PACT-mediated activation of PKR by the herpes simplex virus type 1 Us11 protein. J. Virol. *76*, 11054–11064.

Peters, G.A., Dickerman, B., and Sen, G.C. (2009a). Biochemical analysis of PKR activation by PACT. Biochemistry *48*, 7441–7447.

Peters, G.A., Seachrist, D.D., Keri, R.A., and Sen, G.C. (2009b). The double-stranded RNA-binding protein, PACT, is required for postnatal anterior pituitary proliferation. Proc. Natl. Acad. Sci. USA *106*, 10696–10701.

Pichlmair, A., Schulz, O., Tan, C.P., Näslund, T.I., Liljeström, P., Weber, F., and Reis e Sousa, C. (2006). RIG-I-mediated antiviral responses to single-stranded RNA bearing 5′-phosphates. Science *314*, 997–1001.

Poeck, H., Bscheider, M., Gross, O., Finger, K., Roth, S., Rebsamen, M., Hannesschläger, N., Schlee, M., Rothenfusser, S., Barchet, W., et al. (2010). Recognition of RNA virus by RIG-I results in activation of CARD9 and inflammasome signaling for interleukin 1β production. Nat. Immunol. *11*, 63–69.

Rehwinkel, J., Tan, C.P., Goubau, D., Schulz, O., Pichlmair, A., Bier, K., Robb, N., Vreede, F., Barclay, W., Fodor, E., and Reis e Sousa, C. (2010). RIG-I detects viral genomic RNA during negative-strand RNA virus infection. Cell *140*, 397–408.

Rowe, T.M., Rizzi, M., Hirose, K., Peters, G.A., and Sen, G.C. (2006). A role of the double-stranded RNA-binding protein PACT in mouse ear development and hearing. Proc. Natl. Acad. Sci. USA *103*, 5823–5828.

Satoh, T., Kato, H., Kumagai, Y., Yoneyama, M., Sato, S., Matsushita, K., Tsujimura, T., Fujita, T., Akira, S., and Takeuchi, O. (2010). LGP2 is a positive regulator of RIG-I- and MDA5-mediated antiviral responses. Proc. Natl. Acad. Sci. USA *107*, 1512–1517.

Schlee, M., Hartmann, E., Coch, C., Wimmenauer, V., Janke, M., Barchet, W., and Hartmann, G. (2009a). Approaching the RNA ligand for RIG-I? Immunol. Rev. *227*, 66–74.

Schlee, M., Roth, A., Hornung, V., Hagmann, C.A., Wimmenauer, V., Barchet, W., Coch, C., Janke, M., Mihailovic, A., Wardle, G., et al. (2009b). Recognition of 5′ triphosphate by RIG-I helicase requires short blunt double-stranded RNA as contained in panhandle of negative-strand virus. Immunity *31*, 25–34.

Schmidt, A., Schwerd, T., Hamm, W., Hellmuth, J.C., Cui, S., Wenzel, M., Hoffmann, F.S., Michallet, M.-C., Besch, R., Hopfner, K.-P., et al. (2009). 5′-triphosphate RNA requires base-paired structures to activate antiviral signaling via RIG-I. Proc. Natl. Acad. Sci. USA *106*, 12067–12072.

Schröder, M., Baran, M., and Bowie, A.G. (2008). Viral targeting of DEAD box protein 3 reveals its role in TBK1/IKKε-mediated IRF activation. EMBO J. *27*, 2147–2157.

Schulz, O., Pichlmair, A., Rehwinkel, J., Rogers, N.C., Scheuner, D., Kato, H., Takeuchi, O., Akira, S., Kaufman, R.J., and Reis e Sousa, C. (2010). Protein kinase R contributes to immunity against specific viruses by regulating interferon mRNA integrity. Cell Host Microbe *7*, 354–361.

Siu, K.L., Kok, K.H., Ng, M.H.J., Poon, V.K.M., Yuen, K.Y., Zheng, B.J., and Jin, D.Y. (2009). Severe acute respiratory syndrome coronavirus M protein inhibits type I interferon production by impeding the formation of TRAF3·TANK·TBK1/IKKε complex. J. Biol. Chem. *284*, 16202–16209.

Tabara, H., Yigit, E., Siomi, H., and Mello, C.C. (2002). The dsRNA binding protein RDE-4 interacts with RDE-1, DCR-1, and a DExH-box helicase to direct RNAi in *C. elegans*. Cell *109*, 861–871.

Takahasi, K., Yoneyama, M., Nishihori, T., Hirai, R., Kumeta, H., Narita, R., Gale, M., Jr., Inagaki, F., and Fujita, T. (2008). Nonself RNA-sensing mechanism of RIG-I helicase and activation of antiviral immune responses. Mol. Cell *29*, 428–440.

Yoneyama, M., Kikuchi, M., Natsukawa, T., Shinobu, N., Imaizumi, T., Miyagishi, M., Taira, K., Akira, S., and Fujita, T. (2004). The RNA helicase RIG-I has an essential function in double-stranded RNA-induced innate antiviral responses. Nat. Immunol. *5*, 730–737.

Zeng, W., Sun, L., Jiang, X., Chen, X., Hou, F., Adhikari, A., Xu, M., and Chen, Z.J. (2010). Reconstitution of the RIG-I pathway reveals a signaling role of unanchored polyubiquitin chains in innate immunity. Cell *141*, 315–330.

Zhang, B., Li, M., Chen, L., Yang, K., Shan, Y., Zhu, L., Sun, S., Li, L., and Wang, C. (2009). The TAK1-JNK cascade is required for IRF3 function in the innate immune response. Cell Res. *19*, 412–428.

Zhou, R., Czech, B., Brennecke, J., Sachidanandam, R., Wohlschlegel, J.A., Perrimon, N., and Hannon, G.J. (2009). Processing of *Drosophila* endo-siRNAs depends on a specific Loquacious isoform. RNA *15*, 1886–1895.